Planetary and Space Science 60 (2012) 18–25

Contents lists available at ScienceDirect

Planetary and Space Science

journal homepage: www.elsevier.com/locate/pss

A newly discovered impact crater in Titan's Senkyo: *Cassini* VIMS observations and comparison with other impact features

B.J. Buratti [a,*], C. Sotin [a], K. Lawrence [a], R.H. Brown [b], S. Le Mouélic [c], J.M. Soderblom [b], J. Barnes [d], R.N. Clark [e], K.H. Baines [f], P.D. Nicholson [g]

[a] Jet Propulsion Laboratory, Mail stop 183-401, Pasadena, CA 91109, USA
[b] Dept. Planet. Sci and LPL, U. of AZ, Tucson, AZ 85721-0092, USA
[c] Laboratoire de Planétologie et Géodynamique, CNRS, UMR 6112, Université de Nantes, France
[d] University of Idaho, Department of Physics, Moscow, ID 83844, USA
[e] USGS, Mail Stop 964, Box 25046, Denver Federal Center, Denver, CO 80225, USA
[f] SSEC University of Wisconsin, Madison, WI 53706, USA
[g] Department of Astronomy, Cornell University, Ithaca, NY 14853, USA

ARTICLE INFO

Article history:
Received 10 September 2010
Received in revised form
29 April 2011
Accepted 3 May 2011
Available online 25 May 2011

Keywords:
Titan
Surfaces
Craters

ABSTRACT

Senkyo is an equatorial plain on Titan filled with dunes and surrounded by hummocky plateaus. During the Titan targeted flyby T61 on August 25, 2009, the *Cassini* Visual and Infrared Mapping Spectrometer (VIMS) onboard the *Cassini* spacecraft observed a circular feature, centered at 5.4° N and 341°W, that superimposes the dune fields and a bright plateau. This circular feature, which has been named Paxsi by the International Astronomical Union, is 120 ± 10 km in diameter (measured from the outer edge of the crater rim) and exhibits a central bright area that can be interpreted as the central peak or pit of an impact crater. Although there are only a handful of certain impact craters on Titan, there are two other craters that are of similar size to this newly discovered feature and that have been studied by VIMS: Sinlap (Le Mouélic et al., 2008) and Selk (Soderblom et al., 2010). Sinlap is associated with a large downwind, fan-like feature that may have been formed from an impact plume that rapidly expanded and deposited icy particles onto the surface. Although much of the surrounding region is covered with dunes, the plume region is devoid of dunes. The formation process of Selk also appears to have removed (or covered up) dunes from parts of the adjacent dune-filled terrain. The circular feature on Senkyo is quite different: there is no evidence of an ejecta blanket and the crater itself appears to be infilled with dune material. The rim of the crater appears to be eroded by fluvial processes; at one point the rim is breached. The rim is unusually narrow, which may be due to mass wasting on its inside and subsequent infill by dunes. Based on these observations, we interpret this newly discovered feature to be a more eroded crater than both Sinlap and Selk. Paxsi may have formed during a period when Titan was warmer and more ductile than it is currently.

1. Introduction

Impact craters provide clues to the chronology and general geophysical processes at work on planetary surfaces. The moons of the Solar System range from those with surfaces saturated with impact craters, such as Callisto and the highlands of the Moon, to intermediate cases such as Ganymede, Dione, and Tethys, to those that are crater-free or virtually so, such as Io, Europa, Triton, and the geologically active regions of Enceladus. In the case of Titan, where geologic processes have altered or obliterated many of its craters (Lorenz et al., 2007), the recognition and analysis of impact craters offers a rich storehouse of clues to the existence and persistence of fluvial events, cyrovolcanism, eolian processes, mass wasting, slumping due to viscous relaxation, and other forms of erosion. The study of Titan's craters also yields insights into the comparative study of impact cratering: the surface of Titan may have unique rheological properties that make parts of its surface more ductile, as at least parts of its surface appear to be impregnated with liquid (Lorenz et al., 2006), and Titan is the only icy moon in the Solar System with a substantial atmosphere.

The *Cassini–Huygens* mission provided the first clear view of Titan's surface at high resolution (its nitrogen–methane atmosphere and associated photochemically generated hazes prevented observation of its surface by *Voyager 1* in 1981). Over 70 targeted flybys of the moon in the nominal and extended missions – the count is expected be 126 by the end of the Solstice

* Corresponding author. Tel.: +18183547427.
E-mail address: bonnie.j.buratti@jpl.nasa.gov (B.J. Buratti).

0032-0633/$ - see front matter © 2011 Elsevier Ltd. All rights reserved.
doi:10.1016/j.pss.2011.05.004

Mission in 2017 – and the Huygens probe in January 2005 returned valuable imaging and spectroscopic data. Detailed studies of craters on Titan have been published by the *Cassini* radar team (Elachi et al., 2005; Lorenz et al., 2007; Lopes et al., 2010; Wood et al., 2010). At least five certain impact craters, with 44 more probable ones, have been identified on Titan. As a class, Titan's craters are highly degraded, with evidence of submersion in seas and covering by dunes, as well as the forms of erosion mentioned above (Wood et al., 2010). The high-albedo regions of Titan, in particular Xanadu, tend to be rougher and more heavily cratered (Buratti et al., 2006; Wood et al., 2010).

The *Cassini* Visual Infrared Mapping Spectrometer (VIMS) is an imaging spectrometer covering the 0.4–5.1 μm spectral range with resolution up to 11 nm (higher in the visible), a nominal spatial resolution of 0.5 mrad, and a high-resolution mode of 0.25 mrad in one spatial direction (Brown et al., 2004). For the spatial resolution of the images used in this study see Table 1. Several methane absorption windows in the 1–5 um region offer a view of the surface of Titan, and enable the placement of geologic features within the context of multispectral measurements (e.g., Sotin et al., 2005; McCord et al., 2008). Two of the five definite craters, Selk and Sinlap, have been studied in detail by VIMS (Le Mouélic et al., 2008; Soderblom et al., 2010); the other three, Ksa, Menrva, and Afekan, have not been closely observed by VIMS (Radar and VIMS cannot observe at the same time because of operational considerations). This paper presents an analysis of a circular feature, which we believe to be a third crater, named Paxsi by the International Astronomical Union, that exhibits a strikingly different morphology from the other two craters observed by VIMS, despite their similar sizes. This crater was discovered on August 25, 2009 during the 61st targeted flyby (T61) of the western Senkyo region near Aaru and was imaged by VIMS at a spatial resolution of 18 km/pixel. Fig. 1 shows a VIMS image of the feature obtained at 2.01 μm; the feature is 120 ± 10 km in diameter including its rim and is located at 5.4°N and 341°W. It is circular to within our measurement errors. The width of the crater's outer rim is 25 ± 3 km, and the central peak is 50 ± 10 km in diameter. We note that our images cannot determine whether the central feature is a peak or a pit, but for simplicity we refer to it as a peak. This crater has not been observed by Radar, and unfortunately it will not be observed by Radar in the *Cassini* Solstice Mission (the extended extended mission).

The two impact craters previously observed in detail by VIMS are Sinlap (Le Mouélic et al., 2008) and Selk (Soderblom et al., 2010). The observation of these craters by the Radar instrument on different flybys enabled the acquisition of complementary data on their topography, dielectric constant, and surface roughness. Both craters exhibit morphologic similarities to craters on other moons, with well-formed ejecta blankets (Wood et al., 2010) and central peaks, although Sinlap's is tentatively identified from one pixel in the VIMS data (Le Mouélic et al., 2008). A fan extending from Sinlap, which is about 80 km in diameter and is located at 11°N and 16°W, is hypothesized to have formed by an expanding plume of volatile-rich ejecta mobilized and vaporized by the impact (Le Mouélic et al., 2008). Selk is the geologically younger crater (Le Mouélic et al., 2008; Soderblom et al., 2010) and the crater observed by VIMS at the highest resolution: during T35, T38, and T40 it was imaged at scales up to 2.5 km/pixel. This crater is ~90 km in diameter and is located at 7°N and 199°W in the Belet sand sea. It has a bright rim and evidence for a complex geologic history, including terraced walls and a bench-like structure that extends several hundred kilometers from the crater

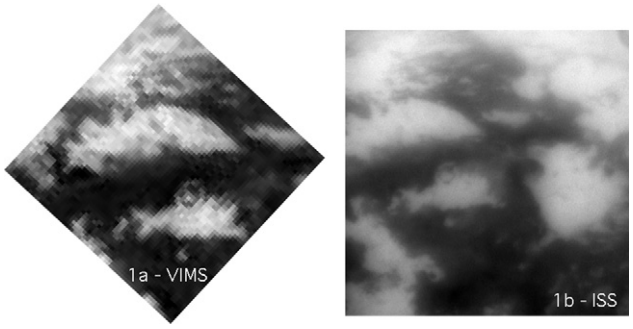

Fig. 1. (a) The VIMS image (at 2.01 μm) from T61 showing the circular feature Paxsi in western Senkyo, which is most likely an impact crater. This image was obtained at a solar phase angle of 12° and a scale of 18 km/pixel. (b) The ISS image obtained at the same time.

Table 1
Observations used in this study.

VIMS Cube ID	Size	Flyby	Central pixel (32,32) geometry						
			Lat. (deg.)	Long. (W deg.)	Phase (deg.)	Incid. (deg.)	Emis. (deg.)	Resolution	
								Smpl (km/px)	Line (km/px)
CM_1629916783	64 × 64	T61	−8.0	337.6	12.9	12.9	0.1	51.6	51.6
CM_1629915961	64 × 64	T61	−8.1	337.1	12.8	12.8	0.1	48.3	48.3
CM_1629915665	64 × 64	T61	−8.1	336.9	12.8	12.8	0.1	46.8	46.8
CM_1629909140	64 × 64	T61	8.7	331.6	12.8	10.4	18.2	29.9	29.9
CM_1629908689	64 × 64	T61	−19.8	0.2	10.9	39.6	29.3	31.4	31.4
CM_1629907554	64 × 64	T61	−39.3	348.1	10.4	44.8	35.0	30.0	30.0
CM_1629906607	64 × 64	T61	−22.4	298.7	12.3	34.0	36.7	22.2	22.2
CM_1629906107	64 × 64	T61	−10.6	332.3	11.6	13.2	1.7	20.5	20.5
CM_1629905607	64 × 64	T61	0.2	0.0	11.1	35.5	32.0	19.5	19.5
CM_1629905033	64 × 64	T61	8.4	344.9	12.0	22.0	24.2	18.0	18.0
CM_1629904536	64 × 64	T61	4.6	334.9	12.1	11.5	16.0	16.6	16.6
CM_1629904033	64 × 64	T61	−1.4	314.6	12.5	9.6	18.4	15.4	15.4
CM_1629903533	64 × 64	T61	−2.3	296.0	13.1	28.1	36.4	14.7	14.7
CM_1629903114	64 × 64	T61	0.8	288.3	13.7	35.6	44.8	13.9	13.9
CM_1629902614	64 × 64	T61	14.9	299.2	14.6	28.3	41.4	13.4	13.4
CM_1629902114	64 × 64	T61	18.6	318.4	14.9	19.1	34.0	11.7	11.7
CM_1629901612	64 × 64	T61	20.1	333.8	15.9	22.3	37.4	10.5	10.5
CM_1629916783	64 × 64	T61	−8.0	337.6	12.9	12.9	0.1	51.6	51.6
CM_1629915961	64 × 64	T61	−8.1	337.1	12.8	12.8	0.1	48.3	48.3

(Soderblom et al., 2010). In spite of its young age, the crater has already shown evidence for both fluvial and eolian erosion (Soderblom et al., 2010), and encroachment by dunes (Lorenz and Radebaugh, 2009).

During the *Cassini* Solstice Mission (2010–2017) additional observations of impact craters, particularly those for which both VIMS and Radar data are available, will offer an opportunity to accomplish comparative studies on the morphology and evolution of craters, enabling a view of how craters evolve from freshly created to highly eroded, and an understanding of the relative importance of various erosional processes through time on Titan.

2. Data analysis

The VIMS data for this work were obtained during the T61 targeted flyby of Titan, which occurred on August 29, 2009, with the closest approach of 961 km. The primary goal of this flyby was to obtain high-resolution Radar SAR images of Titan's equatorial region, including stereo images (with T8) of the Belet sand sea. VIMS was the prime instrument from about 45 min after the closest approach to 2 h and 20 min later to observe western Senkyo and Aaru at small phase angles ($\sim 12^{\circ}$) at a variety of resolutions as well as to monitor clouds (none were identified). The VIMS image cubes were calibrated to units of I/F, where I is the specific intensity (Chandrasekhar, 1960) and πF is the incoming solar flux, with the procedures described by Brown et al. (2004) and augmented by improvements based on the inflight performance of the VIMS instrument. Table 1 lists the observations used in this analysis. Because of the small solar phase angle for these observations and the lack of a change in the viewing geometry on different regions of the crater, no correction for differential atmospheric absorption was needed. (For very large solar phase angles, even a small change in the viewing geometry could cause a substantially different path length for atmospheric scattering and absorption.)

Fig. 2 shows the VIMS mosaic at 2.01 μm of the observations executed within the hour after the closest approach on T61. Of the methane absorption bands centered near 0.93, 1.07, 1.27, 1.59, 2.01, 2.73, and 4.93 μm, 2.01 μm represents the best combination of low atmospheric and haze opacity and sensitivity of the VIMS instrument to yield the best view of the surface. Color maps are most effectively created by first constructing spectral ratios, and then placing these in the RBG color channels. These ratios cancel out illumination differences (which are negligible over the range of the impact crater), and enhance subtle spectral differences, particularly if the wavelengths chosen are at the absorption bands of major surface components as well as in methane windows. Previous work by the VIMS Team has shown that the following three ratios (in μm) of $R=1.59/1.27$, $G=2.03/1.27$, and $B=1.27/1.08$, which are placed near the relatively broad water ice absorption bands at 2.0, 1.56, and 1.25 μm, respectively, are the most sensitive for detecting the relative abundance of water ice and organics on the surface (Sotin et al., 2005; Rodriguez et al., 2006; Barnes et al., 2006, 2007, 2008, 2009; Le Mouélic et al., 2008). These ratios clearly delineate the three major terrains on Titan—high albedo; low albedo possibly enriched in water ice; and dune-rich low albedo (Soderblom et al., 2007, 2010; Le Mouélic et al., 2008). Fig. 3 shows the mosaic of the T61 observations with this color scheme: the dune-rich, low-albedo terrains are brown; the low-albedo terrains possibly enriched in water ice are blue; and the high-albedo terrains are white.

In addition to creating multispectral mosaics of the region of the new crater, we extracted full VIMS spectra from each identifiable feature on the crater and compared these spectra to those of adjacent terrains to understand the relationship of the crater to its surroundings. Fig. 4 shows the categories from which spectra were extracted: adjacent high-albedo regions, adjacent dune-rich low-albedo regions, adjacent low-albedo regions devoid of dunes, the crater floor, the crater central peak and the crater rim. Fig. 5 shows the spectra extracted from all regions. The surface is seen only in the methane windows centered near 0.93, 1.07, 1.27, 1.59, 2.01, 2.73, and 4.93 μm. The spectral band at 4.93 μm is nearly free of haze, so the spectral albedo there is that of the surface. The bright regions (Fig. 5A) and crater rim (Fig. 5B) and central peak (Fig. 5C) have albedos at this band in the range of 0.028–0.060, while the dark areas, both dune covered and not (Fig. 5D and E), exhibit albedos between 0.015 and 0.020.

Our data do not possess sufficient spatial resolution and signal-to-noise in the haze-free 5 μm region to determine the fractional coverage of dunes in the crater floor; however drawing

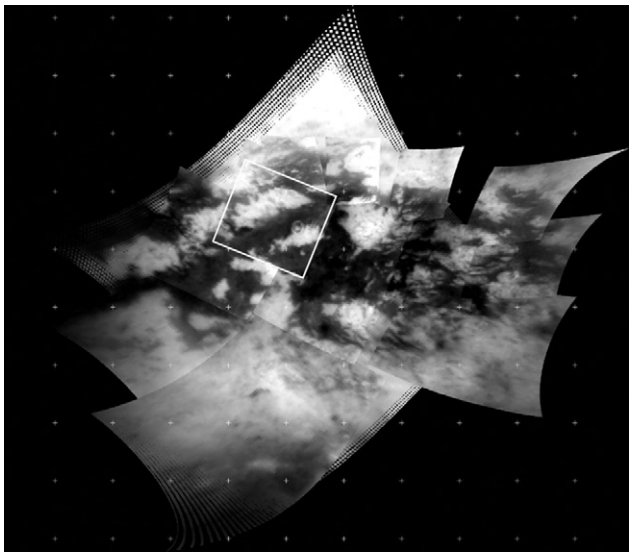

Fig. 2. A mosaic of the entire VIMS observational sequence, which started 45 min after the closest approach. The details of the images used in this mosaic are listed in Table 1. The square figure outlines the VIMS cube in Fig. 4, from which spectra were extracted.

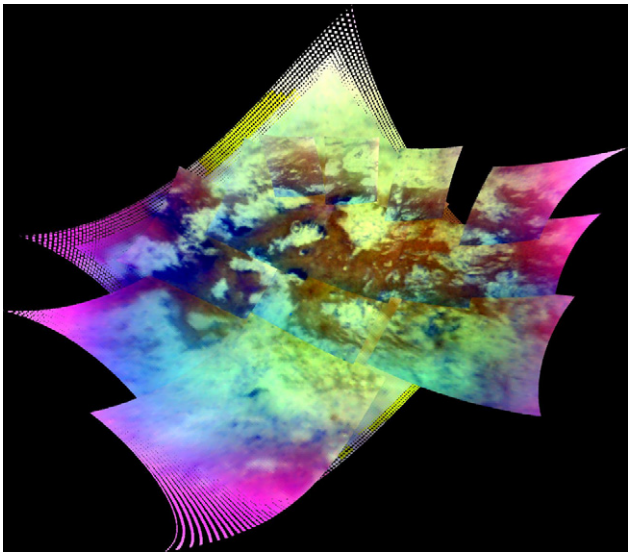

Fig. 3. A color mosaic of the observation shown in Fig. 2. We have used the following scheme for the three channels: $R=1.59/1.27$, $G=2.03/1.27$, and $B=1.27/1.08$. Dune-filled areas are brownish while ice-rich low-albedo regions devoid of dunes appear bluish. (For interpretation of the references to color in this figure legend, the reader is referred to the web version of this article.)

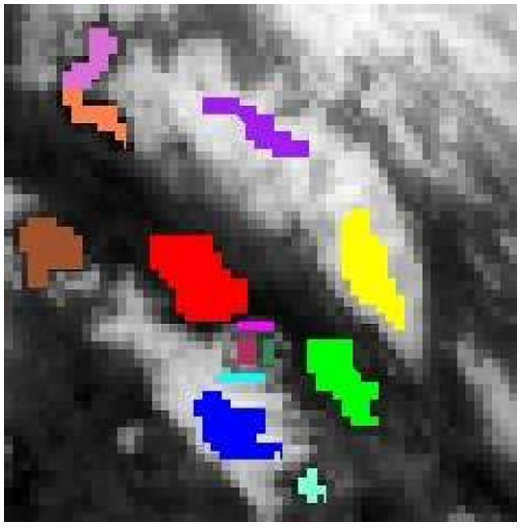

Fig. 4. Paxsi and its surroundings from which spectra were extracted. This image includes the as-yet-unnamed bright region that includes the crater and that lies just above the center of the previous mosaic. The adjacent bright region and parts of the lower albedo Senkyo/Aaru are also included. The main regions are surrounding high-albedo areas (yellow, purple, and blue); low-albedo dune-filled units (lime green and red); low-albedo regions devoid of dunes (lilac, coral, sienna, and the cyan off-crater); crater rim (lilac and cyan); central peak (maroon); and crater floor (dark green). (For interpretation of the references to color in this figure legend, the reader is referred to the web version of this article.)

comparisons to the previous results of the VIMS team described in Barnes et al. (2008) can set reasonable limits on the coverage. For spectral albedos in the 4.93 μm band, which view the surface, Barnes et al. (2008) found similar contrasts between bright and dark areas to ours. The bright equatorial regions in the Barnes et al. study had albedos of 0.05–0.06, while those of the dunes were ~0.03. "Interdune" areas (which our data cannot resolve, but which presumably are spectrally similar to the dune-free dark regions) exhibited intermediate albedos of 0.04–0.05. Because our dune areas – including the area on the crater floor – are at least as dark as those of Barnes et al., and the bright areas are comparable in albedo, we deduce that the dune coverage in the crater is at least as dense as that described by Barnes et al. (2008), which ranged up to full coverage by dunes. We are fairly confident that our dune areas are not just plain sand, as previous studies have shown that every orange region (see Fig. 3) that was seen by Radar revealed dunes to be there (Soderblom et al., 2007). Nevertheless, our resolution is not sufficiently high to directly observe dunes, and Radar has not, and will not, have the opportunity to image dunes in the regions surrounding Paxsi. Thus, our identification of the orange regions in Fig. 3 with dunes is a reasonable extrapolation from previous studies.

Since spectral variations on Titan are subtle, they can be detected best in spectral ratios. The most important spectral differences to study are the relationship of the crater floor, rim, and central peak to the surrounding terrains, including bright areas, dune-free dark areas, and dune-filled dark areas. Fig. 6 is a

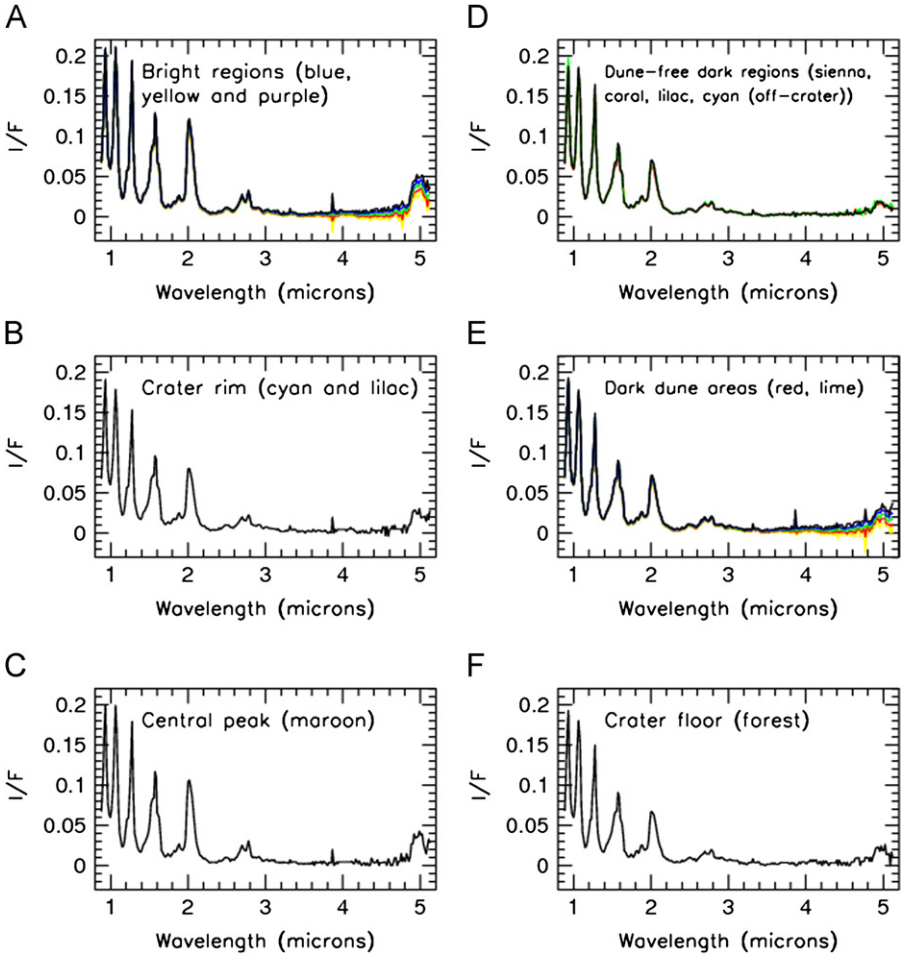

Fig. 5. Examples of full VIMS spectra from 0.93 to 5.1 μm extracted from the image cube. These spectra represent all the major terrain types near the crater.

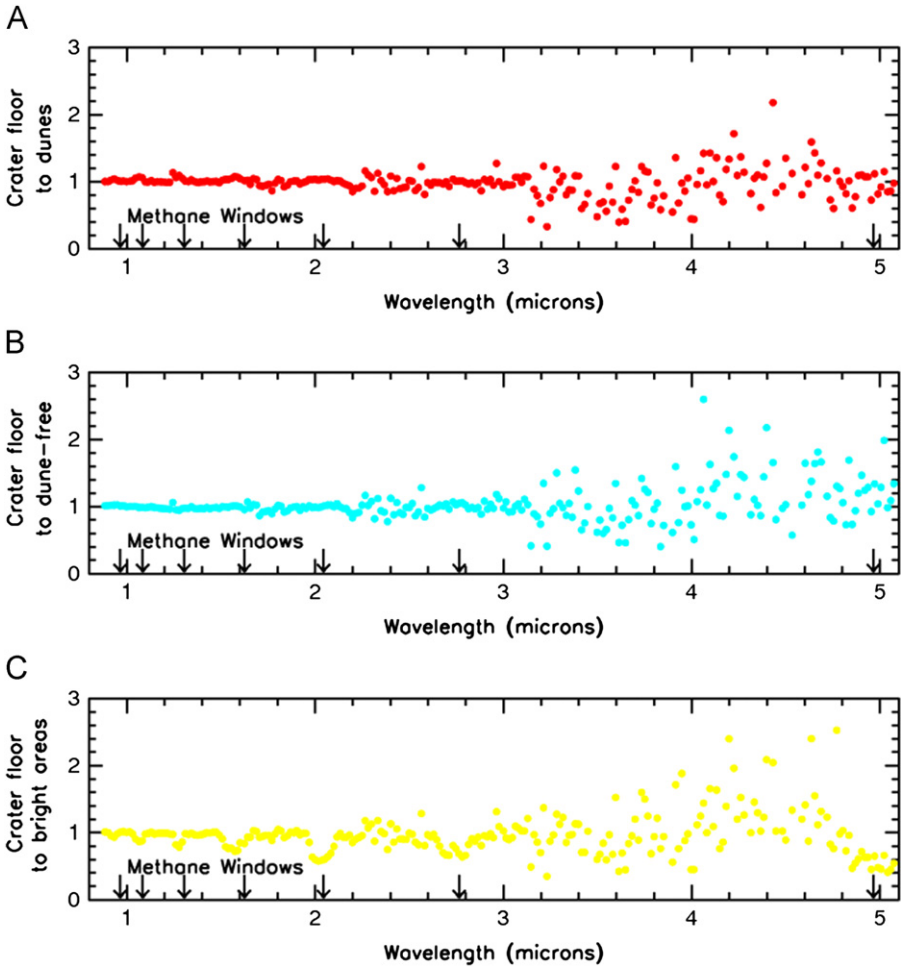

Fig. 6. Ratios of the co-added spectra of the crater floor to three terrains: dune-filled low albedo regions; dune-free low albedo regions; and bright areas. The crater floor is virtually identical to the dunes, but it is higher in the 3–5 μm spectral region when compared to dune-free areas. The water ice absorption bands visible through methane windows are also substantially deeper for the crater floor (see the text for details).

ratio of the crater floor to all three surrounding terrains, showing that the floor is slightly more similar to the dune-rich terrain, specifically in the 3–5 μm area. The crater floor is slightly brighter in this spectral region when compared to the dune-free regions. This result is consistent with the floor being filled with hydrocarbon-rich dunes, which are brighter than water ice in this spectral region. This result is more clearly shown in the mosaic in Fig. 3, where the brownish dune rich terrain dominates the crater floor. The ratio of the crater floor to the bright surrounding areas exhibits absorptions in the methane windows – where water ice absorptions also occur – to show that the crater floors are richer in ice than the surrounding bright terrains. If simple assumptions are made about the nature of the ice on the surface, such as its placement in a checkerboard fashion rather than in an intimate mixture, and no change in particle sizes, we can make estimates of the relative ice abundances in the various terrains. A deep water ice band is fortuitously placed at the 2 μm methane window. Based on the depth of this band (Fig. 6C), the crater floor has $70 \pm 10\%$ more water ice than the surrounding bright areas, a result that suggests the floor may consist partly of water ice that was exposed during the excavation process. Similar ratios for the rim (Fig. 7C) show an enrichment of about $25 \pm 5\%$ for the rim compared to the surrounding bright areas, which also suggests this area may contain particles of excavated ice. On the other hand, the crater rim is depleted in water ice when compared to the dune-rich dark regions (by a factor of $27 \pm 3\%$; see Fig. 7A) and dune-poor dark regions (by a factor of $61 \pm 3\%$; see Fig. 7B). This result suggests that these low albedo regions contain ice particles in addition to the organic-rich sand-like particles mentioned by Barnes et al. (2008). Our results also confirm the enrichment of water ice in the low-albedo dune-free terrain (Soderblom et al., 2007). Finally, a comparison of the central peak with the other terrain types shows it has no measureable spectral differences with the surrounding bright material (Fig. 8C), suggesting they are similar in composition. Like the rim, the central peak is depleted in water ice compared to the dune-filled terrain (Fig. 8A) and dune-free terrain (Fig. 8B) by a factor of $50 \pm 5\%$.

3. Discussion and comparison with other craters

The new crater Paxsi, ~120 km in diameter, crosscuts a bright plateau and a region of low-albedo, hummocky, dune-rich terrain in western Senkyo near Aaru. Paxsi is marked by a large central peak with a diameter nearly half that of the crater, and with a rim that is unusually narrow. In comparison, Selk has a smaller central peak, only ~0.2–0.3 times the crater diameter, not including the rim (Soderblom et al., 2010; see Fig. 8) and Sinlap has, at most, a remnant central peak (Le Mouélic et al., 2008). The only other craters on Titan with comparable central peaks are Ksa, which is smaller ($D = 30$ km) and another unnamed one 63 km in diameter (Wood et al., 2010).

Craters exhibit characteristic features that define both the nature of the impacting body and the substrate into which it

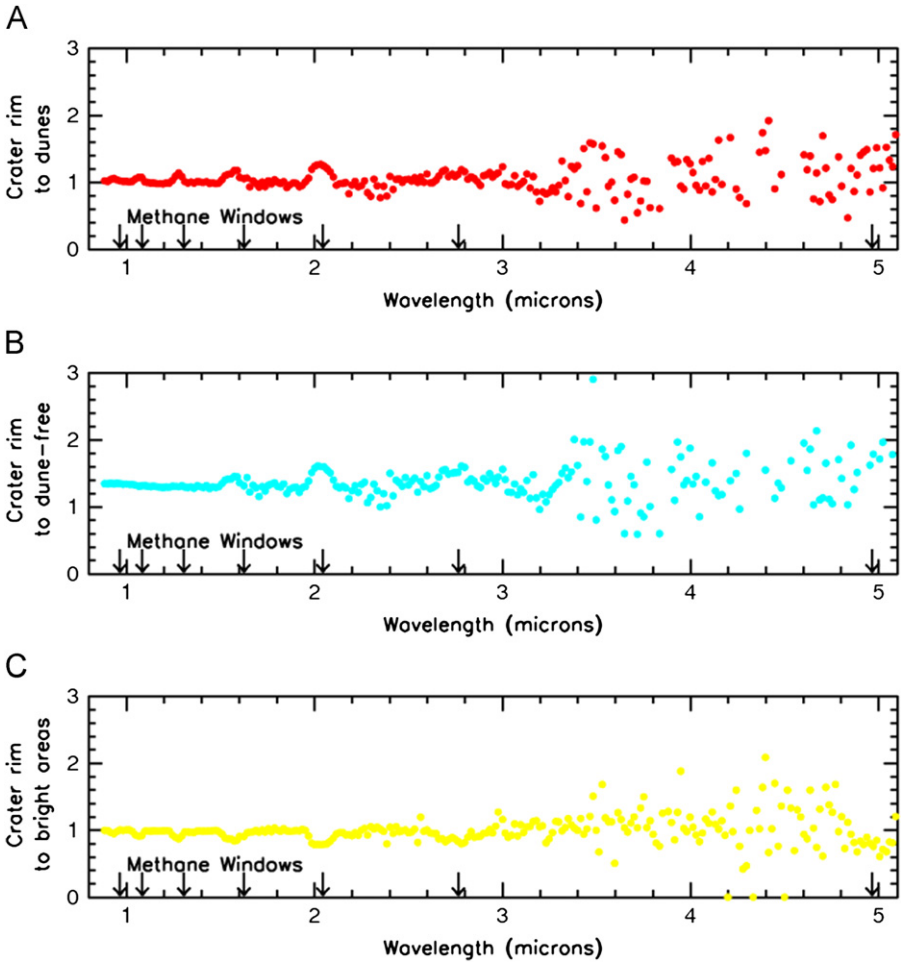

Fig. 7. The ratio of the crater rim to the same three terrains: dune-filled low albedo regions; dune-free low albedo regions; and bright areas. The central rim is depleted in water ice compared to dune-filled and low-albedo dune-free areas, a finding that is consistent with ice particles being mixed in with the dune particles. On the other hand, the crater rim is richer in ice, which suggests it is covered with ice excavated during the formation event.

collides. Both small and large craters have rims that consist of ejected material and define the limits of the disrupted and excavated portion of the impact. The formation of complex craters entails the creation of additional morphological features. One of the most important is a central peak that is due to rebound and subsequent uplift of the crater floor within minutes of the impact event (see Melosh, 1989). Paxsi's large central peak (or pit) may be due to its placement at the interface between two terrains, a region of possible crustal weakness. Alternatively, Titan may in general have a much more ductile or disrupted crust that is conducive to central pit formation. Schenk (1993) found that the central pit morphology of Ganymede and Callisto implied that the mechanical integrity of their crusts was much less than that of the Moon. Another possibility is that during the crater's formation Titan was hotter and more ductile than it was during the formation of more recent craters such as Sinlap and Selk. Ganymede and Callisto, the two icy satellites most comparable to Titan, have many craters dating from earlier epochs, and these tend to have more pronounced central features that approach 0.30 the crater diameter, although the largest craters (>50 km) have central pits rather than peaks (Schenk, 1993). A simpler explanation is that the size of the central peak is just related to the size of the crater. Paxsi is about 1.5 the size of Sinlap and a third larger than Selk. For Ganymede, the size of central peaks for craters comparable to Paxsi is about 0.30–0.40 of the crater diameter, but for smaller Sinlap-sized craters it is only about 0.20 of the diameter (Schenk, 1993). For Titan, both the central peak and the rims of Paxsi, which contain material either excavated or uplifted from the interior, appear to be similar to the surrounding high albedo regions. This result suggests that the high albedo regions may be related to the upper, underlying crust of Titan.

The enrichment of ice for the crater rim, peak, and floor suggests that subsurface ice was excavated during the formation process and still persists on the surface. Paxsi is circular within our measurement errors, which is consistent with formation by a bolide impacting at a non-oblique angle to the surface (Melosh et al., 1989).

There is no hint of a region adjacent to the crater that is devoid of dunes, as is seen at both Sinlap (Le Mouélic et al., 2008) and Selk (Soderblom et al., 2010). Dunes have not only encroached on the crater, but they have entered the crater floor to fill in at least the northern half of the crater floor (see Figs. 3 and 9). Infilling of the crater by dunes and other eolian deposits could also partly explain why the crater's rim is so narrow: dunes may have encroached up the side of the crater. Mass wasting of the rim and subsequent burial by wind-blown deposits may have further contributed to the rim's erosion. Both VIMS and ISS images show that the rim also appears to have been completely breached in its northeast section, possibly by fluvial erosion. Some of the possible craters in Wood et al.'s (2010) survey show similarly narrow rims that could have been subjected to the same erosional processes. One important consideration in drawing comparisons between erosional processes on different craters is whether the rate of

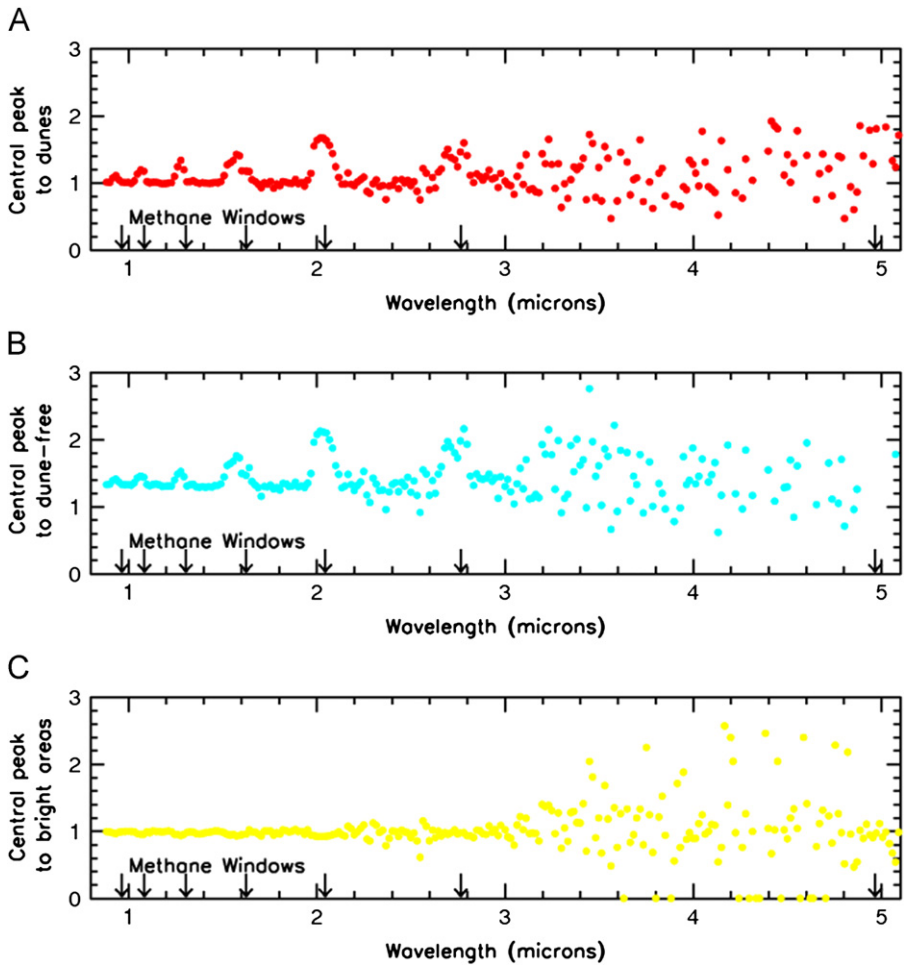

Fig. 8. The ratio of the crater peak (or pit) to the same three terrains: dune-filled low albedo regions; dune-free low albedo regions; and bright areas. As the case for the rim, the central peak is depleted in water ice compared to the dune-filled and low-albedo dune-free areas, but even more substantially. The central peak shows no spectral differences with the surrounding bright areas, suggesting they are similar in composition.

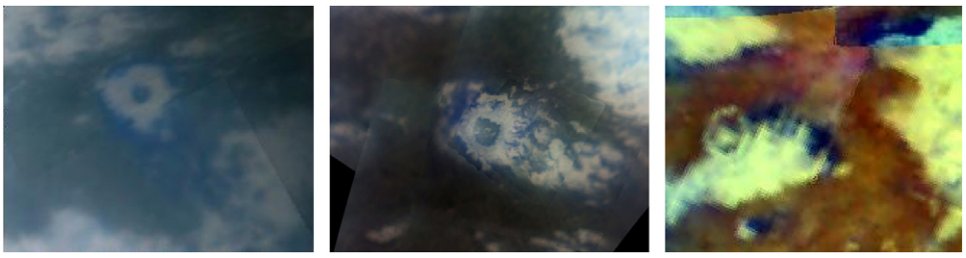

Fig. 9. A comparison of Sinlap (from Le Mouélic et al. (2008)), Selk (from Soderblom et al. (2010)) and Paxsi. Different color schemes were used in the two previous papers, but the dune-free low albedo regions appear as light blue in all the schemes. (For interpretation of the references to color in this figure legend, the reader is referred to the web version of this article.)

erosion is similar at the various sites. Eolian processes, as revealed by the presence of dunes and associated features, dominate the regions $\pm 30^{\circ}$ of the equator (Radebaugh et al., 2008). Since Paxsi, Selk, and Sinlap have relatively similar latitudes (5°, 7°, and 11°, respectively) that are all within this range, eolian erosion should be comparable. The importance of fluvial erosion at various geographical locations is more difficult to quantify. Titan's lakes, which should be associated with the most intense fluvial processes, are in the north polar region. Channels seem to be widely distributed in latitude, and many may be below the resolution limit of the *Cassini* instruments (Lopes et al. 2010). In the equatorial regions where all three craters seen by VIMS lie, it may be local topography that mainly determines fluvial processes.

Paxsi exhibits other marked differences with the Sinlap and Selk. Although the spatial resolution of VIMS images obtained in T61 was nearly an order of magnitude less than that of the highest resolution obtained for Selk, and slightly less than that for Sinlap (14 km/pixel), Paxsi appears to have none of the complex bench-type features seen adjacent to Selk or fan-shaped clearing of dunes emanating from the crater (see Fig. 9). Selk's "bench" is an area of high-albedo terrain that extends beyond the crater. This terrain may be a streamlined upland similar to the islands that form in the large outflow channels of Mars, or it may be a fluidized ejecta flow (Soderblom et al., 2010). If Paxsi had such a region it has eroded away, or it may have been covered up by another material, including eolian deposits.

4. Conclusions

The three craters on Titan so far studied by VIMS at high resolution yield snapshots of progressively eroded features. The least eroded, presumably the youngest, is Selk, with a large bright ejecta blanket surrounded by areas devoid of dunes. Sinlap is more eroded, but it still has a bright prominent rim. Both objects have fan-like features extending from them; presumably they are a remnant of the impact process. No such feature survives in the vicinity of Paxsi. Both less eroded craters do exhibit evidence for nascent erosion: Selk, for example, has a fluted rim due to eolian erosion and prominent fluvial features on the east side of its rim (Soderblom et al., 2010; see Fig. 8). The prominence of erosional features on even relatively fresh-appearing presumably young impact craters speaks to the currently dynamic nature of Titan's surface.

The emplacement of Paxsi in Senkyo suggests that it damaged the hummocky plateau, which must be older, preexisting terrain. Then, the dunes filled the impact crater. Eolian and fluvial processes are at a more advanced stage at Paxsi, appearing to have buried most of the crater rim and breaching its wall in at least one place. Dunes have marched into the northern section of the crater's floor. The Radar survey of five definite craters and 44 crater candidates shows that eolian processes, fluvial erosion, mass wasting, and submersion in seas are the main forces causing the demise of impact craters (Wood et al., 2010). We see no specific evidence for erosion by standing fluids, but the other forms of erosion are all evident. The unusually narrow crater rim is possibly due to mass wasting in its interior and subsequent burial by dunes or wind-blown particles. One outstanding morphological feature of Paxsi is its unusually large central peak: its diameter of 50 ± 10 km is nearly half the size of the crater itself. Craters with central pits comparable in relative size (0.30–0.40 of the crater diameter) are seen on Ganymede (Schenk, 1993), which suggest the feature may be a pit rather than a peak. The peak's (or pit's) large size may be due to crustal weakness at the interface of the Senkyo plain and the bright feature adjacent to the crater. Since a central peak is formed when a pulverized material lacking tensile strength returns to gravitational equilibrium (Melosh, 1989), any preexisting weaknesses would decrease the final tensile strength and enhance this process. Another factor may have been a warmer, more ductile Titan in the past.

Speculations and alternate interpretations of the origin of Paxsi can be entertained. For example, this unusual crater was formed right at the interface between two terrains. The bench-like structure extending from Selk is largely high-albedo terrain and appears to be related in some way to the crater. Could the high albedo region adjacent to Paxsi have been formed, say by cryovolcanism, subsequent to the impact? We simply do not have enough information to answer this question. Is the new crater something other than an impact feature (the IAU cataloged it as a "circular feature")? With a nearly perfect circular structure, and a well-formed rim and central feature, it is difficult to see how it could be anything else, although it is possible that part of the rim is really part of the adjacent high-albedo feature. One important point is that even though the few craters analyzed on Titan show morphological similarities to craters on other icy bodies, the erosional processes acting on them, which are primarily fluvial and eolian, are more like those important on the Earth.

The best analyses of Titan's geologic features come from combining VIMS and Radar data (Soderblom et al., 2007). Unfortunately there are no radar flybys of this region and none planned; the area faces away from Saturn and is thus usually observed as an asymptote during a flyby rather than as a closely approached region. However, comparative analysis with other craters to be observed (and discovered) later in the Solstice Mission by both instruments should shed further light on the evolution of impact craters on Titan.

Acknowledgements

This research was carried out at the Jet Propulsion Laboratory, California Institute of Technology under contract to the National Aeronautics and Space Administration, and was sponsored by the *Cassini* project. We thank Ralph Lorenz and two anonymous reviewers for their detailed comments, and Conor Nixon and Ralph Lorenz for editing this special issue.

References

Barnes, J.W., 11 coauthors, 2006. Cassini observations of flow-like features in western Tui Regio, Titan. Geophys. Res. Lett. 33 CiteID L16204.
Barnes, J.W., Brown, R.H., Soderblom, L.A., Buratti, B.J., Sotin, C., Rodriguez, S., Le Mouélic, S., Baines, K.H., Clark, R.N., Nicholson, P.D., 2007. Global-scale surface spectral variations on Titan seen from Cassini/VIMS. Icarus 186, 242–258.
Barnes, J.W., 12 coauthors, 2008. Spectroscopy, morphometry, and photoclinometry of Titan's dunefields from Cassini/VIMS. Icarus 195, 400–414.
Barnes, J.W., 31 coauthors, 2009. VIMS spectral mapping observations of Titan during the Cassini prime mission Spectroscopy, morphometry, and photoclinometry of Titan's dunefields from Cassini/VIMS. Planet. Space Sci. 57, 1950–1962.
Brown, R.H., 21 coauthors, 2004. The Cassini visual and infrared mapping spectrometer (VIMS) investigation. Space Sci. Rev. 115, 111–168.
Buratti, B.J., et al., 2006. Titan: preliminary results on surface properties and photometry from VIMS observations of the early flybys. Planet. Space Sci 54, 1498–1509.
Chandrasekhar, S., 1960. Radiative Transfer. Dover, New York.
Elachi, C., 34 coauthors, 2005. Cassini radar views the surface of Titan. Science 308, 970–974.
Le Mouélic, S., 17 coauthors, 2008. Mapping and interpretation of Sinlap crater on Titan using Cassini VIMS and RADAR data. J. Geophys. Res. 113, E04003. doi:10.1029/JE002965.
Lopes, R.M.C., 25 coauthors, 2010. Distribution and interplay of geologic processes on Titan from Cassini radar data. Icarus 205, 540–558.
Lorenz, R.D., Niemann, H.B., Harpold, D.N., Way, S.H., Zarnecki, J.C., 2006. Titan's damp ground: Constraints on Titan surface thermal properties from the temperature evolution of the Huygens GCMS inlet. Meteorit. Planet. Sci. 41, 1705–1714.
Lorenz, R.D., Radebaugh, J., 2009. Global pattern of Titan's dunes: radar survey from the Cassini prime mission. Geophys. Res. Lett. 36, L03202. doi:10.1029/2008GL036850.
Lorenz, R.D., 12 coauthors, 2007. Titan's young surface: initial impact crater survey by Cassini Radar and model comparisons. J. Geophys. Res. 113, E04003.
McCord, T.B., 13 coauthors, 2008. Titan's surface: search for spectral diversity and composition using the Cassini VIMS investigation. Icarus 194, 212–242.
Melosh, H.J., 1989. Impact Cratering: A Geologic Process. Oxford University Press, New York.
Radebaugh, J., 14 coauthors, 2008. Dunes on Titan observed by Cassini Radar. Icarus 194, 690–703.
Rodriguez, S., 11 coauthors, 2006. Cassini/VIMS hyperspectral observations of the HUYGENS landing site on Titan. Planet. Space Sci. 54, 1510–1523.
Schenk, P., 1993. Central pit and dome craters: exposing the interiors of Ganymede and Callisto. J. Geophys. Res. 98, 7475–7498.
Sotin, C.R., 25 coauthors, 2005. Release of volatiles from a possible cryovolcano from near-infrared imaging of Titan. Nature 435, 786–789.
Soderblom, J.M., 11 coauthors, 2010. Geology of the Selk crater region on Titan from Cassini VIMS observations. Icarus 208, 905–912.
Soderblom, L.A., 26 coauthors, 2007. Correlations between Cassini VIMS spectra and RADAR SAR images: implications for Titan's surface composition and the character of the Huygens Probe Landing Site. Planet. Space Sci. 55, 2025–2036.
Wood, C.A., Lorenz, R., Kirk, R., Lopes, R., Mitchell, K., Stofan, E., the Cassini Radar Team, 2010. Impact Craters on Titan. Icarus 206, 334–344.